Blucher Mechanical Engineering Proceedings
May 2014, vol. 1 , num. 1
www.proceedings.blucher.com.br/evento/10wccm

A MIXED BEAM ELEMENT COMBINING LINKED AND BUBBLE INTERPOLATIONS

S. Gallegos[1], S. Lecona[1]

[1]Department of Civil Engineering, ITESM Campus Monterrey, Av. Eugenio Garza Sada 2501, Monterrey, Nuevo Leon, Mexico, 64849. (sergio.gallegos@itesm.mx)

Abstract. *Beam elements are some of the most used finite elements in structural analysis. Formulations for these types of elements date from the first years of finite element applications; however, there are still some interesting details to be found in their formulations. In our search for accuracy and computational efficiency, different approaches have been taken to formulate them. Cubic Hermite polynomials were used with potential energy to produce the first beam elements, however, it was difficult to formulate plate and shell elements compatible with them. Compatible two noded elements with linear interpolations were devised but they tend to lock in shear forcing us to under integrate the shear stiffness, and still they were not as accurate. In our quest for accuracy other types of variational principles have been used, mainly the Hellinger-Reissner and the Hu-Washizu principles. Hellinger-Reissner beam elements are accurate and efficient but have difficulties when non linear strain driven constitutive relationships are needed to model the material behavior. Hu-Washizu type elements, on the other hand, have no such problem and are therefore excellent candidates for these formulations, but it is difficult to devise adequate stress, strain and displacement interpolations that offer the same accuracy and efficiency. Different alternatives are used to improve the response of the base linear element; two of them are linked interpolations and bubble functions. In this work it is shown how linked interpolations can be used to avoid the shear locking problem, and bubble functions can be used to generate equivalent strain interpolations that improve the accuracy by using a Hu-Washizu type formulation. The resulting element is as efficient and accurate as a Hellinger-Reissner one but has no problem handling strain driven constitutive relationships for the material.*

Keywords: *Hu-Washizu Principle, linked interpolations, bubble functions, beam elements.*

1. INTRODUCTION

Beam elements are some of the most common types of members employed in solid structural analysis, and their computational modeling has been evolving since the earliest days of the finite element method. Stiffness formulations use displacement interpolation functions. Displacement based beam elements were formulated from the potential energy principle or from the virtual work principle using Hermitian interpolation functions. These elements satisfy compatibility but generate only approximate stiffness matrices for non-prismatic beams. Most of

these elements were based on the Euler-Bernoulli theory and are accurate when the curvature and bending moments are proportional. In the presence of nonlinearity, when the curvatures are of higher order than the bending moments, like in a hinge, extreme refinement is needed for an accurate solution [1]. Flexibility methods use force interpolation. These elements are obtained from the complementary potential energy or from the virtual force principle. They have the advantage of exactly representing the flexibility matrix for non-prismatic elements but have problems satisfying compatibility. One of the first formulations of a force based element is the work of Ciampi and Carlesimo [2]. Mixed formulations based on a two field principle of the Hellinger-Reissner type were developed later by several authors. The work of Spacone, Ciampi and Fillipou [3], and Ayoub and Fillipou [4] generalize beam formulations with independent interpolations of force and displacement. These methods offer good accuracy of the flexibility matrix and satisfy compatibility, but have problems incorporating strain driven material models since they use a flexibility approach for the constitutive relationships. Furthermore, these methods do not have a variational consistent structure, and the stress recovery is not clearly stated.

The Hu-Washizu principle allows for a three field formulation combining independent displacement, strain and stress fields. Elements based on this principle satisfy compatibility and are capable of representing independent strain and stress fields. Assumed enhanced strain elements based on this principle have been successful in the solution of several solid mechanics problems because the strain fields are tailored for the specific problems, like incompressibility or deformation in bending dominated problems. The difficulty with its use is in the definition of adequate fields for strain and stress. An example of a beam element formulated with this principle is the one presented by Taylor, Fillipou, Saritas and Auricchio [5] which is equivalent to a Hellinger-Reissner type element but allowing strain driven constitutive relationships for the material. An elegant formulation for assumed enhanced elements based on this principle is the one presented by Kasper and Taylor [6], which will be used in the present work.

In this work the Hu-Washizu principle is used to generate a beam formulation of the Timoshenko type. The element has no locking in shear and is as accurate as the Hellinger-Reissner type elements. In addition, it is consistent in its variational stress recovery. As a contribution of this work, it is shown how the shear locking problem can be eliminated by using linked interpolations [7] and how to increase the accuracy of the linear beam element by using an enhanced strain field equivalent to a bubble function of the rotation field.

In section 2 a brief description of the beam kinematics and the strong form are presented. In section 3, the weak form corresponding to the stationary condition of the Hu-Washizu principle is presented. In section 4, the matrix forms produced by the specific interpolations for displacements, strains and stresses are presented, and the effect of linked interpolations in the stiffness matrix is shown. Specifically, it is shown how linked interpolations make the shear part of the stiffness matrix singular avoiding the locking effect, and how an enhanced strain field equivalent to a rotation bubble function increases the accuracy of the element. Finally, in section 5, numerical examples are presented followed by a conclusion in section 6.

2. BEAM KINEMATICS AND STRONG FORM

We use a Timoshenko type theory assuming that a plane section, initially normal to the longitudinal axis of the beam, remains plane during all the process of deformation but not necessarily orthogonal to it. This allows for shear deformation to be taken into account. In figure (1.a) a lateral view of the beam is shown with the plane XY being a principal plane. Figure (1.b) shows the positive convention for lateral centroidal displacement v_c and transverse section rotation ϕ_{zc}. Displacement and rotation are combined in the generalized displacement vector **u**:

$$\mathbf{u} = \begin{Bmatrix} v_c \\ \phi_{zc} \end{Bmatrix} \tag{1}$$

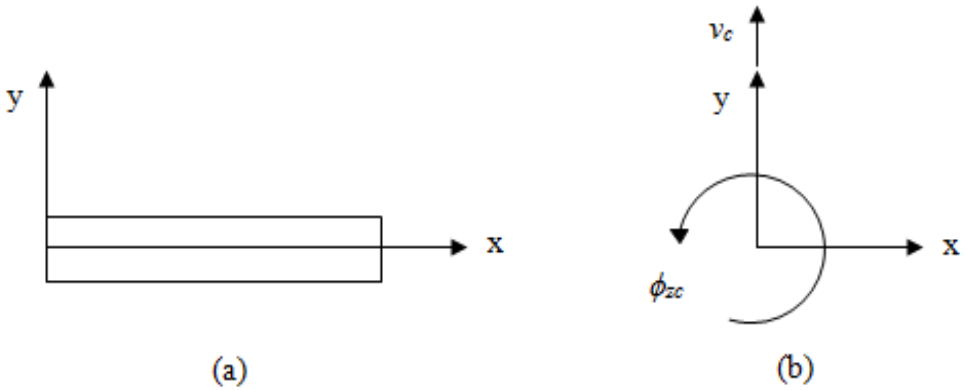

Figure 1. (a) Lateral view of the beam element. (b) Positive displacement and rotation.

Longitudinal displacement of a material particle on a transverse section is expressed as

$$u = -y\phi_{zc} \tag{2}$$

The strain resultant vector $\boldsymbol{\varepsilon}_R$ is composed by the shear strain γ_{xy} and beam curvature κ_{xy}

$$\boldsymbol{\varepsilon}_R = \begin{Bmatrix} \gamma_{xy} \\ \kappa_{xy} \end{Bmatrix} = \begin{Bmatrix} \dfrac{\partial v_c}{\partial x} - \phi_{zc} \\ \dfrac{\partial \phi_{zc}}{\partial x} \end{Bmatrix} = \partial_1 \mathbf{u} \tag{3}$$

The stress resultant vector $\boldsymbol{\sigma}_R$ is formed by the shear force Q_y and the bending moment M_z:

$$\boldsymbol{\sigma}_R = \begin{Bmatrix} Q_y \\ M_z \end{Bmatrix} \tag{4}$$

The shear force and bending moment are defined, respectively by

$$Q_y = \int_A \sigma_{xy} dA,\ M_z = -\int_A \sigma_x y dA \tag{5}$$

Assuming elastic constitutive relationships for the material and combining them with equations (5), we obtain the resultant stress-strain relationships where E is the modulus of elasticity, G the shear modulus, A the transverse section, k_y the shear correction factor and I_z the second moment of inertia.

$$\boldsymbol{\sigma}_R = \mathbf{C}_T \boldsymbol{\varepsilon}_R,\ \mathbf{C}_T = \begin{bmatrix} k_y GA & 0 \\ 0 & EI_z \end{bmatrix}. \tag{6}$$

Figure 2 shows a differential beam element from which the equilibrium equations are obtained:

$$\frac{dQ_y}{dx} + q_y = 0 \tag{7}$$

$$\frac{dM_z}{dx} + Q_y = 0 \tag{8}$$

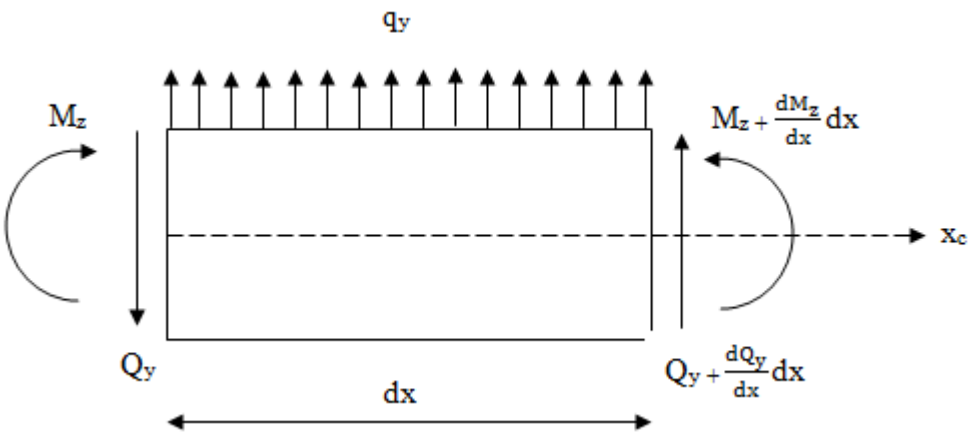

Figure 2. Differential beam element and external loads.

Equations (3) and (6) to (8) state the strong form of the beam problem.

3. THE HU-WASHIZU PRINCIPLE AND THE WEAK FORM.

The three field Hu-Washizu principle may be expressed as:

$$\Pi_{HW(\mathbf{u},\boldsymbol{\varepsilon}_R,\boldsymbol{\sigma}_R)} = \int_{\Omega} W_{R(\mathbf{x},\tilde{\boldsymbol{\varepsilon}}_\mathbf{R})} d\Omega + \int_{\Omega} \boldsymbol{\sigma}_R \cdot \left(\partial_1 \mathbf{u} - \boldsymbol{\varepsilon}_R\right) d\Omega - \int_{\Omega} \mathbf{b} \cdot \mathbf{u} d\Omega - \mathbf{t}_R \cdot \mathbf{u}\Big|_0^L \tag{9}$$

Equation (9) uses a stored strain energy function W_R from which the resultant stress-strain relationship may be obtained

$$\boldsymbol{\sigma}_R = \frac{\partial W_{R(\mathbf{x},\boldsymbol{\varepsilon}_R)}}{\partial \boldsymbol{\varepsilon}_R} \tag{10}$$

Equation (6) is a special case of equation (10) in which the material is linear elastic. Equation (9) contains the external potential energy produced by a body force field **b** and resultant traction vector $\mathbf{t}_R$.

The weak form of the problem is obtained by making the Hu-Washizu principle stationary. **U**, **E** and **S** represent respectively variations of **u**, $\boldsymbol{\varepsilon}$ and $\boldsymbol{\sigma}$. The weak form is split in three parts:

$$\int_L \partial_1 \mathbf{U} \cdot \boldsymbol{\sigma}_R dx - \int_L \mathbf{U} \cdot \mathbf{b} dx - \mathbf{U} \cdot \mathbf{t}_R\Big|_0^L = 0. \tag{11}$$

$$\int_L \mathbf{E} \cdot \left(\frac{\partial W_{R(\mathbf{x},\tilde{\boldsymbol{\varepsilon}}_R)}}{\partial \tilde{\boldsymbol{\varepsilon}}_\mathbf{R}} - \boldsymbol{\sigma}_R \right) dx = 0. \tag{12}$$

$$\int_L \mathbf{S} \cdot \left(\partial_1 \mathbf{u} - \boldsymbol{\varepsilon}_R\right) dx = 0. \tag{13}$$

Following Kasper and Taylor [6], equations (11) and (12) combined collapse into a form similar to the principle of minimum potential energy, and thus will represent the mean for solving the equilibrium equations. Equation (12) will result in an expression to recover post-processing results and (13) will define the enhanced strain, as will be detailed in the next section.

4. THE MATRIX FORM

Interpolation functions for displacement, strain and stress and their variations may be expressed in terms of nodal displacements $\bar{\mathbf{u}}$ and $\bar{\mathbf{U}}$, and indeterminate coefficients $\boldsymbol{\beta}_0$, $\boldsymbol{\beta}_1$, $\boldsymbol{\gamma}_0$, $\boldsymbol{\gamma}_1$, $\boldsymbol{\alpha}$ and $\bar{\boldsymbol{\beta}}_0$, $\bar{\boldsymbol{\beta}}_1$, $\bar{\boldsymbol{\gamma}}_0$, $\bar{\boldsymbol{\gamma}}_1$, $\bar{\boldsymbol{\alpha}}$:

$$\mathbf{u} = \mathbf{N}\bar{\mathbf{u}},\ \boldsymbol{\sigma}_R = \boldsymbol{\beta}_0 + \mathbf{P}\boldsymbol{\beta}_1,\ \boldsymbol{\varepsilon}_R = \boldsymbol{\gamma}_0 + \mathbf{Q}\boldsymbol{\gamma}_1 + \mathbf{R}\boldsymbol{\alpha} \tag{14}$$

$$\mathbf{U} = \mathbf{N}\bar{\mathbf{U}},\ \mathbf{S} = \bar{\boldsymbol{\beta}}_0 + \mathbf{P}\bar{\boldsymbol{\beta}}_1,\ \mathbf{E} = \bar{\boldsymbol{\gamma}}_0 + \mathbf{Q}\bar{\boldsymbol{\gamma}}_1 + \mathbf{R}\bar{\boldsymbol{\alpha}} \tag{15}$$

Following [6], equation (13) is transformed into an equivalent expression for the resultant strain which is obtained as:

$$\boldsymbol{\varepsilon}_R = \mathbf{B}_u \bar{\mathbf{u}} + \mathbf{B}_\alpha \boldsymbol{\alpha} \tag{16}$$

Where

$$\mathbf{B}_u = \mathbf{B}_\Omega + \mathbf{Q}\mathbf{G}^{-1}\mathbf{g} \text{ and } \mathbf{B}_\alpha = \mathbf{R} \tag{17}$$

$$\mathbf{B}_\Omega = \frac{1}{L}\int_L \mathbf{B}dx \text{ and } \mathbf{B} = \partial_1 \mathbf{N} \tag{18}$$

$$\mathbf{G} = \int_L \mathbf{P}^T \mathbf{Q} dx \text{ and } \mathbf{g} = \int_L \mathbf{P}^T \left(\mathbf{B} - \mathbf{B}_\Omega\right) dx \tag{19}$$

From equation (12) the resultant stress is recovered by evaluating the coefficients as:

$$\boldsymbol{\beta}_0 = \frac{1}{L}\int_L \frac{\partial W_{R(\mathbf{x},\boldsymbol{\varepsilon}_R)}}{\partial \boldsymbol{\varepsilon}_R} dx \text{ and } \boldsymbol{\beta}_1 = \mathbf{G}^{-1}\mathbf{h} \tag{20}$$

With

$$\mathbf{h} = \int_L \mathbf{Q}^T \left[\frac{\partial W_{R(\mathbf{x},\boldsymbol{\varepsilon}_R)}}{\partial \boldsymbol{\varepsilon}_R} - \boldsymbol{\beta}_0\right] dx\,. \tag{21}$$

Finally, by combining equations (11) and (12), but using the definition of the resultant strain (16), a set of stiffness equations is obtained which can be solved by using a Newton-Raphson approach. Coefficients $\boldsymbol{\alpha}$ may be condensed out if necessary since they are not continuous between elements.

$$\begin{Bmatrix} \mathbf{F}_{\text{int}} - \mathbf{F}_{ext} \\ \mathbf{F}_{enh} \quad \mathbf{0} \end{Bmatrix}_{(\bar{\mathbf{u}}^0, \boldsymbol{\alpha}^0)} + \begin{bmatrix} \mathbf{k}_{uu} & \mathbf{k}_{u\alpha} \\ \mathbf{k}_{\alpha u} & \mathbf{k}_{\alpha\alpha} \end{bmatrix} \begin{Bmatrix} d\bar{\mathbf{u}} \\ d\boldsymbol{\alpha} \end{Bmatrix} = \mathbf{0} \tag{22}$$

$$\begin{bmatrix} \mathbf{k}_{uu} \\ \mathbf{k}_{\alpha u} \end{bmatrix}_{(\bar{\mathbf{u}}^0, \boldsymbol{\alpha}^0)} = \begin{bmatrix} \int_L \mathbf{B}_u{}^T \mathbf{C}_T \mathbf{B}_u dx \\ \int_L \mathbf{B}_\alpha{}^T \mathbf{C}_T \mathbf{B}_u dx \end{bmatrix} \text{ and } \begin{bmatrix} \mathbf{k}_{u\alpha} \\ \mathbf{k}_{\alpha\alpha} \end{bmatrix}_{(\bar{\mathbf{u}}^0, \boldsymbol{\alpha}^0)} = \begin{bmatrix} \int_L \mathbf{B}_u{}^T \mathbf{C}_T \mathbf{B}_\alpha dx \\ \int_L \mathbf{B}_\alpha{}^T \mathbf{C}_T \mathbf{B}_\alpha dx \end{bmatrix} \tag{23}$$

$$\mathbf{F}_{int} = \int_L (\mathbf{B}_u)^T \left[\frac{\partial W_{R(\mathbf{x},\boldsymbol{\varepsilon}_R)}}{\partial \boldsymbol{\varepsilon}_R}\right] dx \;\; \mathbf{F}_{enh} = \int_L (\mathbf{B}_\alpha)^T \left[\frac{\partial W_{R(\mathbf{x},\boldsymbol{\varepsilon}_R)}}{\partial \boldsymbol{\varepsilon}_R}\right] dx \;\; \mathbf{F}_{ext} = \int_L \mathbf{N}^T \mathbf{b} dx - \mathbf{N}^T \mathbf{t}_R \Big|_0^L \tag{24}$$

Using static condensation on equation (22) the equivalent stiffness matrix and the condensed coefficients are given by

$$\left[\mathbf{k}^{e}\right]^{(k)} = \left[\mathbf{k}^{e}_{uu}\right]^{(k)} - \left[\mathbf{k}^{e}_{u\alpha}\right]^{(k)} \left[\mathbf{k}^{e}_{\alpha\alpha}\right]^{(k)^{-1}} \left[\mathbf{k}^{e}_{\alpha u}\right]^{(k)} \tag{25}$$

$$d\boldsymbol{\alpha}^{e} = -\left[\mathbf{k}^{e}_{\alpha\alpha}\right]^{-1} \left(\mathbf{F}^{e}_{enh} + \mathbf{k}^{e}_{\alpha u} d\bar{\mathbf{u}}^{e}\right) \tag{26}$$

4.1. Linear element with two nodes.

In figure 3 the linear beam element with two nodes implemented in this work is shown.

Figure 3. Beam element with two nodes.

Without considering the enhanced term **R** in the strain field at this moment, the following interpolations are used:

$$\begin{Bmatrix} v_c \\ \phi_{zc} \end{Bmatrix} = \begin{bmatrix} N_1 & 0 & N_2 & 0 \\ 0 & N_1 & 0 & N_2 \end{bmatrix} \begin{Bmatrix} \bar{v}_1 \\ \bar{\phi}_{z1} \\ \bar{v}_2 \\ \bar{\phi}_{z2} \end{Bmatrix} \tag{27}$$

$$\begin{Bmatrix} \gamma_{xy} \\ \kappa_{xy} \end{Bmatrix} = \begin{Bmatrix} \gamma_{01} \\ \gamma_{02} \end{Bmatrix} + \begin{bmatrix} Q_1 & 0 \\ 0 & Q_1 \end{bmatrix} \begin{Bmatrix} \gamma_{11} \\ \gamma_{12} \end{Bmatrix} \tag{28}$$

$$\begin{Bmatrix} Q_y \\ M_z \end{Bmatrix} = \begin{Bmatrix} \beta_{01} \\ \beta_{02} \end{Bmatrix} + \begin{bmatrix} P_1 & 0 \\ 0 & P_1 \end{bmatrix} \begin{Bmatrix} \beta_{11} \\ \beta_{12} \end{Bmatrix} \tag{29}$$

$$N_1 = 1-\xi,\ N_2 = \xi,\ P_1 = Q_1 = \frac{1}{2} - \xi,\ \xi = \frac{x}{L} \tag{30}$$

After inserting (27) through (30) into (25), the following condensed stiffness matrix is obtained:

$$\mathbf{k}^e = k_y GA \begin{bmatrix} \frac{1}{L} & \frac{1}{2} & -\frac{1}{L} & \frac{1}{2} \\ \frac{1}{2} & \frac{L}{3} & -\frac{1}{2} & \frac{L}{6} \\ -\frac{1}{L} & -\frac{1}{2} & \frac{1}{L} & -\frac{1}{2} \\ \frac{1}{2} & \frac{L}{6} & -\frac{1}{2} & \frac{L}{3} \end{bmatrix} + \frac{EI_z}{L} \begin{bmatrix} 0 & 0 & 0 & 0 \\ 0 & 1 & 0 & -1 \\ 0 & 0 & 0 & 0 \\ 0 & -1 & 0 & 1 \end{bmatrix} \tag{31}$$

The first term, which is the shear part, is of order 4 with 2 rigid body modes and full rank 2. The actual rank is 2 and therefore, it will lock when L is large or the beam is thin because the L terms in the matrix will dominate the behavior. The second term, the flexural part is of order 2, with 1 rigid body mode and full rank 1. The actual rank is 1 and it will describe correctly constant curvature.

In order to solve the shear locking problem a quadratic linked interpolation [7] is proposed to enrich the displacement description (27):

$$\begin{Bmatrix} v_c \\ \phi_{zc} \end{Bmatrix} = \begin{bmatrix} N_1 & 0 & N_2 & 0 \\ 0 & N_1 & 0 & N_2 \end{bmatrix} \begin{Bmatrix} \bar{v}_1 \\ \bar{\phi}_{z1} \\ \bar{v}_2 \\ \bar{\phi}_{z2} \end{Bmatrix} + \begin{bmatrix} 0 & N_{v\phi 1} & 0 & N_{v\phi 2} \\ 0 & 0 & 0 & 0 \end{bmatrix} \begin{Bmatrix} \bar{v}_1 \\ \bar{\phi}_{z1} \\ \bar{v}_2 \\ \bar{\phi}_{z2} \end{Bmatrix} \tag{32}$$

$$N_{v\phi 1} = aL\xi(1-\xi), \quad N_{v\phi 2} = aL\xi(\xi - 1) \tag{33}$$

The following shear stiffness is obtained:

$$\mathbf{k}_{shear} = k_y GA \begin{bmatrix} \frac{1}{L} & \frac{1}{2} & -\frac{1}{L} & \frac{1}{2} \\ \frac{1}{2} & (a^2 - a + 1)\frac{L}{3} & -\frac{1}{2} & (-2a^2 + 2a + 1)\frac{L}{6} \\ -\frac{1}{L} & -\frac{1}{2} & \frac{1}{L} & -\frac{1}{2} \\ \frac{1}{2} & (-2a^2 + 2a + 1)\frac{L}{6} & -\frac{1}{2} & (a^2 - a + 1)\frac{L}{3} \end{bmatrix} \tag{34}$$

In order to reduce its rank by one, the coefficients (2,2) and (4,2) are equated giving the value a=1/2. The matrix order is still 4 with 2 rigid body modes and full rank 2, but now the rank is 1, and it will not lock when L is large or the beam is thin. The final stiffness matrix is now:

$$\mathbf{k}^e = k_y GA \begin{bmatrix} \frac{1}{L} & \frac{1}{2} & -\frac{1}{L} & \frac{1}{2} \\ \frac{1}{2} & \frac{L}{4} & -\frac{1}{2} & \frac{L}{4} \\ -\frac{1}{L} & -\frac{1}{2} & \frac{1}{L} & -\frac{1}{2} \\ \frac{1}{2} & \frac{L}{4} & -\frac{1}{2} & \frac{L}{4} \end{bmatrix} + \frac{EI_z}{L} \begin{bmatrix} 0 & 0 & 0 & 0 \\ 0 & 1 & 0 & -1 \\ 0 & 0 & 0 & 0 \\ 0 & -1 & 0 & 1 \end{bmatrix} \tag{35}$$

An alternative procedure to assign a value to the coefficient *a*, consists in computing the shear strain:

$$\gamma_{xy} = \frac{\partial v_c}{\partial x} - \phi_{zc} = \left[\frac{\bar{v}_2 - \bar{v}_2}{L} - a\left(\bar{\phi}_{z2} - \bar{\phi}_{z1}\right) - \bar{\phi}_{z1} \right] + \left(1-2a\right)\xi\bar{\phi}_{z1} - \left(1-2a\right)\xi\bar{\phi}_{z2} \tag{36}$$

With a=1/2 the linear part is eliminated and the shear strain is constant along the element. This was the assumption taken in [7]. The same effect is obtained by taking $\gamma_{xy} = \gamma_{01}$ in (28). Still another alternative to obtain the same result would be to sub integrate with 1 point the expressions for the shear stiffness matrix. They are all equivalent schemes.

With the stiffness matrix given in (35), the beam element will not lock but its accuracy is still not very good, it takes too many elements for the solution to converge to the right values. Therefore, a further improvement is necessary, and it is achieved by introducing an enhanced strain field. This field is obtained by adding a bubble function to the rotation field (32):

$$\begin{Bmatrix} v_c \\ \phi_{zc} \end{Bmatrix} = \begin{bmatrix} N_1 & 0 & N_2 & 0 \\ 0 & N_1 & 0 & N_2 \end{bmatrix} \begin{Bmatrix} \bar{v}_1 \\ \bar{\phi}_{z1} \\ \bar{v}_2 \\ \bar{\phi}_{z2} \end{Bmatrix} + \begin{bmatrix} 0 & N_{v\phi 1} & 0 & N_{v\phi 2} \\ 0 & 0 & 0 & 0 \end{bmatrix} \begin{Bmatrix} \bar{v}_1 \\ \bar{\phi}_{z1} \\ \bar{v}_2 \\ \bar{\phi}_{z2} \end{Bmatrix} + \begin{bmatrix} 0 \\ \xi - \xi^2 \end{bmatrix} \{\delta_1\} \tag{37}$$

It can be demonstrated that the addition of the bubble function in (37) is equivalent to using the following enhanced linear strain field in (28):

$$\begin{Bmatrix} \gamma_{xy} \\ \kappa_{xy} \end{Bmatrix} = \begin{Bmatrix} \gamma_{01} \\ \gamma_{02} \end{Bmatrix} + \begin{bmatrix} Q_1 & 0 \\ 0 & Q_1 \end{bmatrix} \begin{Bmatrix} \gamma_{11} \\ \gamma_{12} \end{Bmatrix} + \begin{bmatrix} -\frac{1}{6} \\ \frac{2}{L}\left(\frac{1}{2} - \xi\right) \end{bmatrix} \{\alpha\} \tag{38}$$

After this enhancement, the final stiffness matrix will not lock in shear and the beam formulation will be very accurate as shown in the examples below.

$$\mathbf{k}^e = \left(\frac{\frac{12EI_z}{L}}{k_y GAL + \frac{12EI_z}{L}} \right) k_y GA \begin{bmatrix} \frac{1}{L} & \frac{1}{2} & -\frac{1}{L} & \frac{1}{2} \\ \frac{1}{2} & \frac{L}{4} & -\frac{1}{2} & \frac{L}{4} \\ -\frac{1}{L} & -\frac{1}{2} & \frac{1}{L} & -\frac{1}{2} \\ \frac{1}{2} & \frac{L}{4} & -\frac{1}{2} & \frac{L}{4} \end{bmatrix} + \frac{EI_z}{L} \begin{bmatrix} 0 & 0 & 0 & 0 \\ 0 & 1 & 0 & -1 \\ 0 & 0 & 0 & 0 \\ 0 & -1 & 0 & 1 \end{bmatrix} \tag{39}$$

It can be shown that equation (39) is completely equivalent to the stiffness matrix proposed in [5] by Taylor, Fillipou, Saritas and Auricchio, which was found in a different way.

5. NUMERICAL EXAMPLES

5.1. Displacement validation: Simply supported beam with uniform load.

Consider the simply supported beam shown in figure 4 with uniform load. The properties of the problem are: $E = 10^6$, $v = 0.25$, $q = 1$, $k = 5/6$, $h = b = 1$. (Taylor et al.[5])

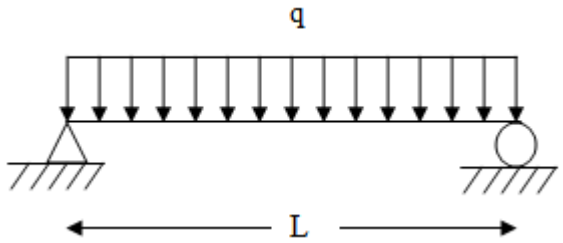

Figure 4. Simply supported beam with uniform load.

The exact solution of the problem using Timoshenko beam theory is:

$$w_{\max} = \frac{5qL^4}{384EI} + \frac{qL^2}{8kGA} \tag{40}$$

$$\theta_{\max} = -\frac{qL^3}{24EI} \tag{41}$$

The problem is modeled with one element using symmetry. Table 1 shows the results of the analysis for different aspect ratios, comparing the formulations of Taylor et al. [5], the one developed by the authors of this paper, based on the Hu-Washizu variational principle, and the one developed by Gallegos [8] under the Hellinger-Reissner variational principle.

Table 1. Maximum displacement and rotation in a simply supported beam under uniform load.

	$L/h = 10$		$L/h = 100$	
	$w_{max} \times 10^{2}$	$\theta_0 \times 10^{-3}$	$w_{max} \times 10^{-2}$	θ_0
Exact solution	0.160000	-0.50000	0.15629	-0.50000
Taylor et al.	0.160000	-0.50000	0.15629	-0.50000
Gallegos and Lecona	0.160000	-0.50000	0.15629	-0.50000
Hellinger-Reissner	0.160000	-0.50000	0.15629	-0.50000

All formulations yield the same results, even for thin beams. No shear locking is observed.

Figure 5 illustrates the effect of the enhanced strain functions presented above on the vertical displacement. Note how remarkable is the improvement in the accuracy, especially for coarse meshes. The factor acting on the shear stiffness matrix in (39) is really important in order to get accurate results.

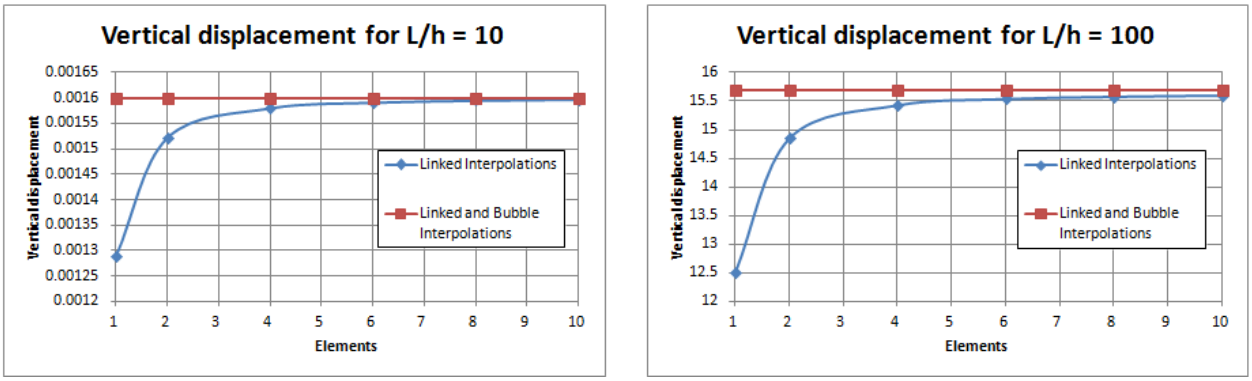

Figure 5. Vertical displacement for beams with different aspect ratios considering linked interpolations and linked and enhanced interpolations.

5.2. Displacement and Force validation: Fixed-fixed beam under uniform load.

Consider the fixed-fixed beam subjected to uniform load shown in figure 6. Properties for the square cross section used are: $E = 47619.04763$, $v = 0.052801058$, $q = -1.0$, $L = 4$.

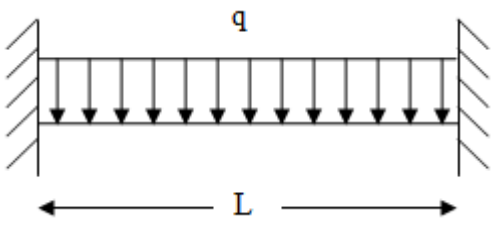

Figure 6. Fixed-fixed beam under uniform load.

A comparison between the Hellinger-Reissner formulation by Gallegos [8] and the authors of this paper is made for maximum vertical displacement and maximum moment as shown in Table 2 and Table 3 respectively. An exact solution of this example is derived for a Timoshenko beam.

Table 2. Maximum vertical displacement in a fixed-fixed beam under uniform load.

	***L/h* = 10**	***L/h* = 100**
	w_{max}	w_{max}
Exact Solution	-0.00722	-65.7
Gallegos and Lecona	-0.00723	-65.7
Hellinger-Reissner	-0.00723	-65.7

Table 3. Maximum moment at beam ends in a fixed-fixed beam under uniform loading.

Maximum Moment				
Elements	***L/h* = 10**		***L/h* = 100**	
	Gallegos and Lecona	**Hellinger-Reissner**	**Gallegos and Lecona**	**Hellinger-Reissner**
2	-1.000	-1.000	-1.000	-1.000
4	-1.250	-1.250	-1.250	-1.250
8	-1.312	-1.312	-1.312	-1.312
16	-1.328	-1.328	-1.328	-1.328
32	-1.332	-1.332	-1.332	-1.332
64	-1.333	-1.333	-1.333	-1.333
Exact solution	-1.333		-1.333	

The estimate of lateral deflection is excellent as can be observed from the results in Table 2. Table 3, on the other hand, shows that a fine mesh is still necessary to capture correctly the maximum moment in the beam. The Hellinger-Reissner formulation and our current Hu-Washizu element are completely equivalent.

5.3. Strain Enhancement: Cantilever beam with uniform load.

Consider the fixed-free beam shown in figure 7. Let the properties of this beam be the same as those used for the first example, that is, $E = 10^6$, $v = 0.25$, $q = 1$, $k = 5/6$, $h = b = 1$.

This example is demonstrates the differences between the Hellinger-Reissner [8] formulation and the current Hu-Washizu one.

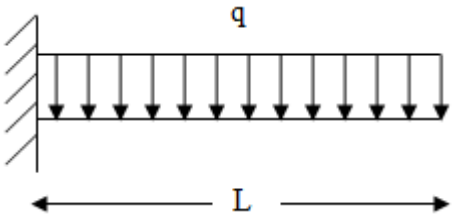

Figure 7. Cantilever beam under uniform load.

Table 4 and Table 5 display the maximum shear distortion and curvature for the two formulations. A considerable improvement is obtained in the Hu-Washizu formulation since the strains are approximated independently, as expected.

Table 4. Maximum distortion in a cantilever beam under uniform loading.

Maximum Distortion γ				
Elements	***L/h* = 10**		***L/h* = 100**	
	Gallegos and Lecona	**Hellinger-Reissner**	**Gallegos and Lecona**	**Hellinger-Reissner**
1	-1.501e-5	-51.5e-5	-1.501e-4	-0.500
2	-2.251e-5	-21.0e-5	-2.251e-4	-0.188
4	-2.626e-5	-8.095e-5	-2.626e-4	-0.055
8	-2.814e-5	-4.278e-5	-2.814e-4	-0.015
16	-2.907e-5	-3.286e-5	-2.907e-4	-4.075e-3
32	-2.954e-5	-3.050e-5	-2.954e-4	-1.257e-3
64	-2.978e-5	-3.002e-5	-2.978e-4	-5.400e-4
100	-2.986e-5	-3.000e-5	-2.986e-4	-3.981e-4

Table 5. Maximum curvature in a cantilever beam under uniform loading.

Maximum Curvature κ				
Elements	***L/h* = 10**		***L/h* = 100**	
	Gallegos and Lecona	**Gallegos**	**Gallegos and Lecona**	**Gallegos**
1	-0.500e-3	-0.200e-3	-0.050	-0.020
2	-0.575e-3	-0.350e-3	-0.058	-0.035
4	-0.594e-3	-0.463e-3	-0.059	-0.046
8	-0.598e-3	-0.528e-3	-0.060	-0.053
16	-0.600e-3	-0.563e-3	-0.060	-0.056
32	-0.600e-3	-0.581e-3	-0.060	-0.058
64	-0.600e-3	-0.591e-3	-0.060	-0.059
100	-0.600e-3	-0.594e-3	-0.060	-0.059

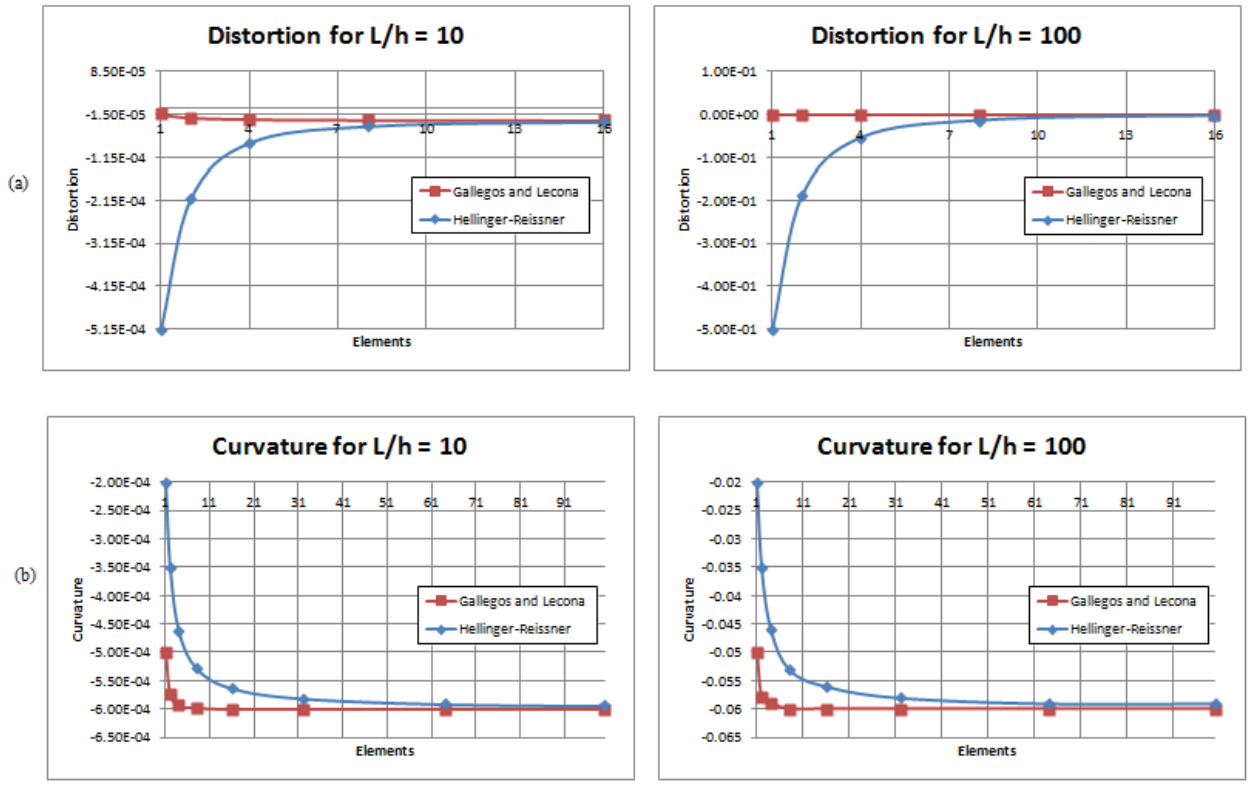

Figure 8. Convergence for strain results in a cantilever beam under uniform loading. (a) shows shear distortion convergence and (b) curvature convergence.

In Figure 8, the difference in convergence between the Hellinger-Reissner [8] and the current Hu-Washizu formulation is shown. Again, a considerable improvement is observed as a consequence of the independent interpolation for the strains. This effect is more important in coarse meshes. Since in the Hu-Washizu formulation the strains are described by linear fields, softer plots for strains can be obtained in comparison with the constant values obtained in [8], as shown in Figure 9.

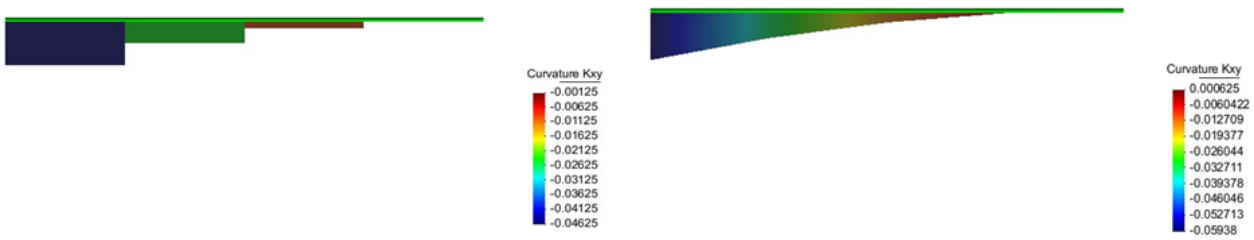

(a) (b)

Figure 9. Curvature in a cantilever beam under uniform load for (a) Hellinger-Reissner based formulation (b) Hu-Washizu based formulation.

6. CONCLUSIONS

The formulation and implementation for a linear Timoshenko beam element with two nodes based on the Hu-Washizu principle has been presented in this work. The original element has a problem with shear locking and slow convergence. In order to remedy the locking problem, a linked quadratic interpolation was added to the displacement field linking it to nodal rotations. The linking functions are multiplied by a scale factor, the magnitude of which is adjusted in order to make singular the shear component of the stiffness matrix. This adjustment is equivalent to assuming a constant shear strain along the element or to sub integrate the shear component with one integration point.

The accuracy is improved by enhancing the strain field. One of the difficulties of the three field principle is the right selection of interpolation functions. We have selected here a constant shear and a linear curvature fields which are equivalent to adding a quadratic bubble function to the rotation field. These interpolations produce an additional factor which multiplies the shear stiffness matrix and scales it proportionally to the ratio of flexural stiffness to the sum of shear and flexural stiffness combined. For short span beams, with large shear stiffness and small flexural stiffness, the factor is smaller than the unit and diminishes further the effect of the shear stiffness, while in long span beams, with small shear stiffness and large flexural stiffness, the factor tends to the unit value.

The examples presented in this work show the excellent capacity of this element to describe correctly the displacement, strain and curvature of beams even with coarse meshes. The accuracy of shear and moment on the other hand, still require the use of a fine mesh to reach the correct result.

In summary, the beam element formulated here is accurate even for coarse meshes and does not show locking in shear for thin beams. The form of the constitutive relationship used in the formulation allows strain driven algorithms to be used without any problem. This will allow its use in future work on reinforced concrete prestressed beams.

7. REFERENCES

[1] K.D. Hjelmstad and E. Taciroglu , “Mixed methods and flexibility approaches for nonlinear frame analysis”, *Journal of structural steel research* 58, 967-993, 2002.

[2] Ciampi V. and Carlesimo L., “A nonlinear beam element for seismic analysis of structures”, *Proc. European Conference on Earthquake Engineering, Lisbon, Portugal*, 73-80, 1986.

[3] Spacone E., Ciampi V. and Fillipou F.C., “Mixed formulation of nonlinear beam finite element”, *Computers & Structures*, 1, 71-83, 1996.

[4] Ayoub A.S. and Fillipou F.C., “Mixed formulation of nonlinear steel-concrete composite beam element”, *J. of Structural Engineering*, 126(3), 371-381, 2000.

[5] Taylor R.L., Fillipou F.C. Saritas A. and Auricchio F., “A mixed finite element method for beam and frame problems”, *Computational Mechanics*, 31, 192-203, 2003.

[6] Kasper E.P. and Taylor R.L., “A mixed enhanced strain method, Part I: Geometrically linear problems”, *Computers & Structures*, 75, 237-250, 2000.

[7] Zienkiewicz O.C., Xu, Zeng, Samuelsson, Wiberg., “Linked Interpolation for Reissner-Mindlin plate elements: Part I- A simple quadrilateral”, *International Journal For Numerical Methods In Engineering*, 36, 3043-3056, 1993.

[8] Gallegos S., “Análisis de sólidos y estructural mediante el método de elementos finitos”, *Limusa, México*, 2008.